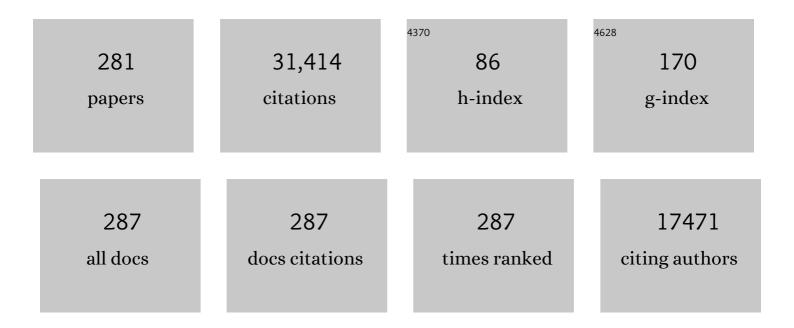
List of Publications by Year in descending order

Source: https://exaly.com/author-pdf/9074380/publications.pdf Version: 2024-02-01



IIA-OINC HE

#	Article	IF	CITATIONS
1	High-performance bulk thermoelectrics with all-scale hierarchical architectures. Nature, 2012, 489, 414-418.	13.7	3,767
2	All-solid-state dye-sensitized solar cells with high efficiency. Nature, 2012, 485, 486-489.	13.7	1,608
3	Ultrahigh power factor and thermoelectric performance in hole-doped single-crystal SnSe. Science, 2016, 351, 141-144.	6.0	1,594
4	Strained endotaxial nanostructures with high thermoelectric figure of merit. Nature Chemistry, 2011, 3, 160-166.	6.6	911
5	3D charge and 2D phonon transports leading to high out-of-plane <i>ZT</i> in n-type SnSe crystals. Science, 2018, 360, 778-783.	6.0	859
6	All-scale hierarchical thermoelectrics: MgTe in PbTe facilitates valence band convergence and suppresses bipolar thermal transport for high performance. Energy and Environmental Science, 2013, 6, 3346.	15.6	646
7	High-entropy-stabilized chalcogenides with high thermoelectric performance. Science, 2021, 371, 830-834.	6.0	546
8	BiCuSeO oxyselenides: new promising thermoelectric materials. Energy and Environmental Science, 2014, 7, 2900-2924.	15.6	544
9	Broad temperature plateau for thermoelectric figure of merit ZT>2 in phase-separated PbTe0.7S0.3. Nature Communications, 2014, 5, 4515.	5.8	461
10	High Performance Thermoelectrics from Earth-Abundant Materials: Enhanced Figure of Merit in PbS by Second Phase Nanostructures. Journal of the American Chemical Society, 2011, 133, 20476-20487.	6.6	433
11	High performance bulk thermoelectrics via a panoscopic approach. Materials Today, 2013, 16, 166-176.	8.3	421
12	High thermoelectric performance in low-cost SnS _{0.91} Se _{0.09} crystals. Science, 2019, 365, 1418-1424.	6.0	395
13	Tuning Multiscale Microstructures to Enhance Thermoelectric Performance of nâ€Type Bismuthâ€Tellurideâ€Based Solid Solutions. Advanced Energy Materials, 2015, 5, 1500411.	10.2	379
14	Unit-cell scale mapping of ferroelectricity and tetragonality in epitaxial ultrathin ferroelectric films. Nature Materials, 2007, 6, 64-69.	13.3	368
15	High thermoelectric performance of oxyselenides: intrinsically low thermal conductivity of Ca-doped BiCuSeO. NPG Asia Materials, 2013, 5, e47-e47.	3.8	349
16	A high thermoelectric figure of merit ZT > 1 in Ba heavily doped BiCuSeO oxyselenides. Energy and Environmental Science, 2012, 5, 8543.	15.6	333
17	Texturation boosts the thermoelectric performance of BiCuSeO oxyselenides. Energy and Environmental Science, 2013, 6, 2916.	15.6	326
18	High Performance Na-doped PbTe–PbS Thermoelectric Materials: Electronic Density of States Modification and Shape-Controlled Nanostructures. Journal of the American Chemical Society, 2011, 133, 16588-16597.	6.6	322

#	Article	IF	CITATIONS
19	Origin of the High Performance in GeTe-Based Thermoelectric Materials upon Bi ₂ Te ₃ Doping. Journal of the American Chemical Society, 2014, 136, 11412-11419.	6.6	319
20	High Thermoelectric Performance Realized in a BiCuSeO System by Improving Carrier Mobility through 3D Modulation Doping. Journal of the American Chemical Society, 2014, 136, 13902-13908.	6.6	317
21	Raising the Thermoelectric Performance of p-Type PbS with Endotaxial Nanostructuring and Valence-Band Offset Engineering Using CdS and ZnS. Journal of the American Chemical Society, 2012, 134, 16327-16336.	6.6	308
22	Microstructure‣attice Thermal Conductivity Correlation in Nanostructured PbTe _{0.7} S _{0.3} Thermoelectric Materials. Advanced Functional Materials, 2010, 20, 764-772.	7.8	307
23	Enhanced atomic ordering leads to high thermoelectric performance in AgSbTe ₂ . Science, 2021, 371, 722-727.	6.0	306
24	Ultrahigh thermoelectric performance in Cu ₂ Se-based hybrid materials with highly dispersed molecular CNTs. Energy and Environmental Science, 2017, 10, 1928-1935.	15.6	298
25	High performance n-type Ag2Se film on nylon membrane for flexible thermoelectric power generator. Nature Communications, 2019, 10, 841.	5.8	291
26	Origin of low thermal conductivity in SnSe. Physical Review B, 2016, 94, .	1.1	287
27	Nanostructures Boost the Thermoelectric Performance of PbS. Journal of the American Chemical Society, 2011, 133, 3460-3470.	6.6	282
28	Power generation and thermoelectric cooling enabled by momentum and energy multiband alignments. Science, 2021, 373, 556-561.	6.0	270
29	Enhanced Thermoelectric Properties in the Counter-Doped SnTe System with Strained Endotaxial SrTe. Journal of the American Chemical Society, 2016, 138, 2366-2373.	6.6	269
30	Synergistically optimized electrical and thermal transport properties of SnTe via alloying high-solubility MnTe. Energy and Environmental Science, 2015, 8, 3298-3312.	15.6	268
31	Low-cost, abundant binary sulfides as promising thermoelectric materials. Materials Today, 2016, 19, 227-239.	8.3	257
32	Realizing record high performance in n-type Bi ₂ Te ₃ -based thermoelectric materials. Energy and Environmental Science, 2020, 13, 2106-2114.	15.6	249
33	High-Performance Solution-Processed Amorphous Zincâ^'Indiumâ^'Tin Oxide Thin-Film Transistors. Journal of the American Chemical Society, 2010, 132, 10352-10364.	6.6	235
34	Thermoelectrics with Earth Abundant Elements: High Performance p-type PbS Nanostructured with SrS and CaS. Journal of the American Chemical Society, 2012, 134, 7902-7912.	6.6	233
35	High figure-of-merit and power generation in high-entropy GeTe-based thermoelectrics. Science, 2022, 377, 208-213.	6.0	233
36	Remarkable Roles of Cu To Synergistically Optimize Phonon and Carrier Transport in n-Type PbTe-Cu ₂ Te. Journal of the American Chemical Society, 2017, 139, 18732-18738.	6.6	230

#	Article	IF	CITATIONS
37	On the Origin of Increased Phonon Scattering in Nanostructured PbTe Based Thermoelectric Materials. Journal of the American Chemical Society, 2010, 132, 8669-8675.	6.6	211
38	Extraordinary Thermoelectric Performance Realized in nâ€Type PbTe through Multiphase Nanostructure Engineering. Advanced Materials, 2017, 29, 1703148.	11.1	209
39	Structure of the CED-4–CED-9 complex provides insights into programmed cell death in Caenorhabditis elegans. Nature, 2005, 437, 831-837.	13.7	207
40	Understanding of the Extremely Low Thermal Conductivity in Highâ€Performance Polycrystalline SnSe through Potassium Doping. Advanced Functional Materials, 2016, 26, 6836-6845.	7.8	201
41	Realizing high performance n-type PbTe by synergistically optimizing effective mass and carrier mobility and suppressing bipolar thermal conductivity. Energy and Environmental Science, 2018, 11, 2486-2495.	15.6	200
42	Grain Boundary Engineering for Achieving High Thermoelectric Performance in n‶ype Skutterudites. Advanced Energy Materials, 2017, 7, 1602582.	10.2	194
43	Large enhancement of thermoelectric properties in n-type PbTe via dual-site point defects. Energy and Environmental Science, 2017, 10, 2030-2040.	15.6	194
44	Extraordinary thermoelectric performance in n-type manganese doped Mg3Sb2 Zintl: High band degeneracy, tuned carrier scattering mechanism and hierarchical microstructure. Nano Energy, 2018, 52, 246-255.	8.2	188
45	Superior thermoelectric performance in PbTe–PbS pseudo-binary: extremely low thermal conductivity and modulated carrier concentration. Energy and Environmental Science, 2015, 8, 2056-2068.	15.6	185
46	Potential-Dependent Phase Transition and Mo-Enriched Surface Reconstruction of γ-CoOOH in a Heterostructured Co-Mo ₂ C Precatalyst Enable Water Oxidation. ACS Catalysis, 2020, 10, 4411-4419.	5.5	174
47	Exploring Resonance Levels and Nanostructuring in the PbTeâ^ CdTe System and Enhancement of the Thermoelectric Figure of Merit. Journal of the American Chemical Society, 2010, 132, 5227-5235.	6.6	171
48	Ultrahigh power factor and flexible silver selenide-based composite film for thermoelectric devices. Energy and Environmental Science, 2020, 13, 1240-1249.	15.6	165
49	Thermoelectrics from Abundant Chemical Elements: High-Performance Nanostructured PbSe–PbS. Journal of the American Chemical Society, 2011, 133, 10920-10927.	6.6	164
50	Simultaneous optimization of electrical and thermal transport properties of Bi0.5Sb1.5Te3 thermoelectric alloy by twin boundary engineering. Nano Energy, 2017, 37, 203-213.	8.2	164
51	High thermoelectric figure of merit in nanostructured p-type PbTe–MTe (M = Ca, Ba). Energy and Environmental Science, 2011, 4, 4675.	15.6	162
52	High-entropy enhanced capacitive energy storage. Nature Materials, 2022, 21, 1074-1080.	13.3	161
53	Integrating Band Structure Engineering with All‣cale Hierarchical Structuring for High Thermoelectric Performance in PbTe System. Advanced Energy Materials, 2017, 7, 1601450.	10.2	157
54	Good Performance and Flexible PEDOT:PSS/Cu ₂ Se Nanowire Thermoelectric Composite Films. ACS Applied Materials & Interfaces, 2019, 11, 12819-12829.	4.0	153

#	Article	IF	CITATIONS
55	Controlled heterogeneous water distribution and evaporation towards enhanced photothermal water-electricity-hydrogen production. Nano Energy, 2020, 77, 105102.	8.2	148
56	Enhancing the Figure of Merit of Heavyâ€Band Thermoelectric Materials Through Hierarchical Phonon Scattering. Advanced Science, 2016, 3, 1600035.	5.6	147
57	Strong enhancement of phonon scattering through nanoscale grains in lead sulfide thermoelectrics. NPG Asia Materials, 2014, 6, e108-e108.	3.8	140
58	Functional Monolithic Polymeric Organic Framework Aerogel as Reducing and Hosting Media for Ag nanoparticles and Application in Capturing of Iodine Vapors. Chemistry of Materials, 2012, 24, 1937-1943.	3.2	137
59	Liquid-like thermal conduction in intercalated layered crystalline solids. Nature Materials, 2018, 17, 226-230.	13.3	136
60	Strong Phonon Scattering by Layer Structured PbSnS ₂ in PbTe Based Thermoelectric Materials. Advanced Materials, 2012, 24, 4440-4444.	11.1	130
61	Multiple Converged Conduction Bands in K ₂ Bi ₈ Se ₁₃ : A Promising Thermoelectric Material with Extremely Low Thermal Conductivity. Journal of the American Chemical Society, 2016, 138, 16364-16371.	6.6	130
62	Role of Sodium Doping in Lead Chalcogenide Thermoelectrics. Journal of the American Chemical Society, 2013, 135, 4624-4627.	6.6	128
63	Enhancement of Thermoelectric Figure of Merit by the Insertion of MgTe Nanostructures in <i>p</i> â€ŧype PbTe Doped with Na ₂ Te. Advanced Energy Materials, 2012, 2, 1117-1123.	10.2	123
64	Enhanced mid-temperature thermoelectric performance of textured SnSe polycrystals made of solvothermally synthesized powders. Journal of Materials Chemistry C, 2016, 4, 2047-2055.	2.7	122
65	Synergistic modulation of mobility and thermal conductivity in (Bi,Sb) ₂ Te ₃ towards high thermoelectric performance. Energy and Environmental Science, 2019, 12, 624-630.	15.6	120
66	Attaining high mid-temperature performance in (Bi,Sb)2Te3 thermoelectric materials via synergistic optimization. NPG Asia Materials, 2016, 8, e302-e302.	3.8	119
67	Enhanced thermoelectric performance of PbTe bulk materials with figure of merit zT >2 by multi-functional alloying. Journal of Materiomics, 2016, 2, 141-149.	2.8	118
68	Simultaneously enhancing the power factor and reducing the thermal conductivity of SnTe via introducing its analogues. Energy and Environmental Science, 2017, 10, 2420-2431.	15.6	116
69	Enhanced thermoelectric properties of p-type nanostructured PbTe–MTe (M = Cd, Hg) materials. Energy and Environmental Science, 2013, 6, 1529.	15.6	115
70	Long-Range Ordering of Oxygen-Vacancy Planes in α-Fe ₂ O ₃ Nanowires and Nanobelts. Chemistry of Materials, 2008, 20, 3224-3228.	3.2	112
71	Phonon Scattering and Thermal Conductivity in pâ€Type Nanostructured PbTeâ€BaTe Bulk Thermoelectric Materials. Advanced Functional Materials, 2012, 22, 5175-5184.	7.8	112
72	Highâ€Performance Thermoelectricity in Nanostructured Earthâ€Abundant Copper Sulfides Bulk Materials. Advanced Energy Materials, 2016, 6, 1600607.	10.2	111

#	Article	IF	CITATIONS
73	In Situ Nanostructure Generation and Evolution within a Bulk Thermoelectric Material to Reduce Lattice Thermal Conductivity. Nano Letters, 2010, 10, 2825-2831.	4.5	108
74	Raising thermoelectric performance of n-type SnSe via Br doping and Pb alloying. RSC Advances, 2016, 6, 98216-98220.	1.7	107
75	Highly Enhanced Thermoelectric Properties of Bi/Bi ₂ S ₃ Nanocomposites. ACS Applied Materials & Interfaces, 2017, 9, 4828-4834.	4.0	107
76	Scaling of structure and electrical properties in ultrathin epitaxial ferroelectric heterostructures. Journal of Applied Physics, 2006, 100, 051609.	1.1	106
77	Entropy engineering promotes thermoelectric performance in p-type chalcogenides. Nature Communications, 2021, 12, 3234.	5.8	105
78	Direct observation of vast off-stoichiometric defects in single crystalline SnSe. Nano Energy, 2017, 35, 321-330.	8.2	101
79	High Thermoelectric Performance Achieved in GeTe–Bi ₂ Te ₃ Pseudoâ€Binary via Van der Waals Gapâ€induced Hierarchical Ferroelectric Domain Structure. Advanced Functional Materials, 2019, 29, 1806613.	7.8	101
80	Realizing high-efficiency power generation in low-cost PbS-based thermoelectric materials. Energy and Environmental Science, 2020, 13, 579-591.	15.6	101
81	Morphology Control of Nanostructures: Na-Doped PbTe–PbS System. Nano Letters, 2012, 12, 5979-5984.	4.5	100
82	Boosting the Thermoelectric Performance of Pseudo‣ayered Sb ₂ Te ₃ (GeTe) <i>_n</i> via Vacancy Engineering. Advanced Science, 2018, 5, 1801514.	5.6	95
83	Surface nitridation of nickel-cobalt alloy nanocactoids raises the performance of water oxidation and splitting. Applied Catalysis B: Environmental, 2020, 270, 118889.	10.8	95
84	Seeing Is Believing: Weak Phonon Scattering from Nanostructures in Alkali Metal-Doped Lead Telluride. Nano Letters, 2012, 12, 343-347.	4.5	94
85	Polymer/carbon nanotube composite materials for flexible thermoelectric power generator. Composites Science and Technology, 2017, 153, 71-83.	3.8	92
86	Electronic and Magnetic Properties of Ultrathin Au/Pt Nanowires. Nano Letters, 2009, 9, 3177-3184.	4.5	91
87	Significantly Enhanced Thermoelectric Performance in nâ€ŧype Heterogeneous BiAgSeS Composites. Advanced Functional Materials, 2014, 24, 7763-7771.	7.8	91
88	Remarkable electron and phonon band structures lead to a high thermoelectric performance <i>ZT</i> > 1 in earth-abundant and eco-friendly SnS crystals. Journal of Materials Chemistry A, 2018, 6, 10048-10056.	5.2	90
89	Realizing Highâ€Ranged Outâ€ofâ€Plane ZTs in Nâ€Type SnSe Crystals through Promoting Continuous Phase Transition. Advanced Energy Materials, 2019, 9, 1901334.	10.2	83
90	Advanced electron microscopy for thermoelectric materials. Nano Energy, 2015, 13, 626-650.	8.2	80

#	Article	IF	CITATIONS
91	The Thermoelectric Properties of SnSe Continue to Surprise: Extraordinary Electron and Phonon Transport. Chemistry of Materials, 2018, 30, 7355-7367.	3.2	79
92	Enhanced thermoelectric properties of bismuth telluride bulk achieved by telluride-spilling during the spark plasma sintering process. Scripta Materialia, 2018, 143, 90-93.	2.6	77
93	Preparation and Characterization of Te/Poly(3,4-ethylenedioxythiophene):Poly(styrenesulfonate)/Cu ₇ Te ₄ Ternary Composite Films for Flexible Thermoelectric Power Generator. ACS Applied Materials & Interfaces, 2018. 10. 42310-42319.	4.0	74
94	Multipoint Defect Synergy Realizing the Excellent Thermoelectric Performance of nâ€Type Polycrystalline SnSe via Re Doping. Advanced Functional Materials, 2019, 29, 1902893.	7.8	73
95	High thermoelectric performance in n-type BiAgSeS due to intrinsically low thermal conductivity. Energy and Environmental Science, 2013, 6, 1750.	15.6	68
96	Optical Functional Materials Inspired by Biology. Advanced Optical Materials, 2016, 4, 195-224.	3.6	67
97	Energetics of Nanoparticle Exsolution from Perovskite Oxides. Journal of Physical Chemistry Letters, 2018, 9, 3772-3778.	2.1	65
98	Selective Surfaces: Quaternary Co(Ni)MoS-Based Chalcogels with Divalent (Pb ²⁺ ,) Tj ETQq0 0 0 rgBT Separation. Chemistry of Materials, 2012, 24, 3380-3392.	- /Overlock 3.2	2 10 Tf 50 4 63
99	Enhancing Localized Evaporation through Separated Light Absorbing Centers and Scattering Centers. Scientific Reports, 2015, 5, 17276.	1.6	63
100	New insight into InSb-based thermoelectric materials: from a divorced eutectic design to a remarkably high thermoelectric performance. Journal of Materials Chemistry A, 2017, 5, 5163-5170.	5.2	63
101	Synergistically optimizing thermoelectric transport properties of n-type PbTe via Se and Sn co-alloying. Journal of Alloys and Compounds, 2017, 724, 208-221.	2.8	59
102	A hierarchical carbon nitride tube with oxygen doping and carbon defects promotes solar-to-hydrogen conversion. Journal of Materials Chemistry A, 2020, 8, 3160-3167.	5.2	59
103	High Power Factor Ag/Ag ₂ Se Composite Films for Flexible Thermoelectric Generators. ACS Applied Materials & Interfaces, 2021, 13, 14327-14333.	4.0	58
104	Strategy to optimize the overall thermoelectric properties of SnTe via compositing with its property-counter CulnTe2. Acta Materialia, 2017, 125, 542-549.	3.8	56
105	High thermoelectric figure of merit and improved mechanical properties in melt quenched PbTe–Ge and PbTe–Ge1â^'xSix eutectic and hypereutectic composites. Journal of Applied Physics, 2009, 105, .	1.1	55
106	Synergizing aliovalent doping and interface in heterostructured NiV nitride@oxyhydroxide core-shell nanosheet arrays enables efficient oxygen evolution. Nano Energy, 2021, 85, 105961.	8.2	55
107	PbTe–PbSnS2 thermoelectric composites: low lattice thermal conductivity from large microstructures. Energy and Environmental Science, 2012, 5, 8716.	15.6	54
108	2D hetero-nanosheets to enable ultralow thermal conductivity by all scale phonon scattering for highly thermoelectric performance. Nano Energy, 2016, 30, 780-789.	8.2	54

#	Article	IF	CITATIONS
109	Understanding Nanostructuring Processes in Thermoelectrics and Their Effects on Lattice Thermal Conductivity. Advanced Materials, 2016, 28, 2737-2743.	11.1	54
110	Thermoelectric Properties and Nanostructuring in the p-Type Materials NaPb _{18â^'<i>x</i>} Sn _{<i>x</i>} MTe ₂₀ (M = Sb, Bi). Chemistry of Materials, 2009, 21, 1683-1694.	3.2	53
111	Ion-Exchangeable Cobalt Polysulfide Chalcogel. Journal of the American Chemical Society, 2011, 133, 1200-1202.	6.6	53
112	Enhanced thermoelectric properties of SnSe polycrystals via texture control. Physical Chemistry Chemical Physics, 2016, 18, 31821-31827.	1.3	53
113	Influence of defects on the thermoelectricity in SnSe: A comprehensive theoretical study. Physical Review B, 2018, 97, .	1.1	53
114	Constructing van der Waals gaps in cubic-structured SnTe-based thermoelectric materials. Energy and Environmental Science, 2020, 13, 5135-5142.	15.6	53
115	Hierarchical Self-Assembly of Nanowires on the Surface by Metallo-Supramolecular Truncated Cuboctahedra. Journal of the American Chemical Society, 2021, 143, 5826-5835.	6.6	53
116	Realizing high thermoelectric performance in non-nanostructured n-type PbTe. Energy and Environmental Science, 2022, 15, 1920-1929.	15.6	53
117	First-Principles Study of Anharmonic Lattice Dynamics in Low Thermal Conductivity <mml:math xmlns:mml="http://www.w3.org/1998/Math/MathML" display="inline"><mml:mrow><mml:msub><mml:mrow><mml:mi>AgCrSe</mml:mi></mml:mrow><mml:mrow>< : Evidence for a Large Resonant Four-Phonon Scattering. Physical Review Letters. 2020. 125. 245901.</mml:mrow></mml:msub></mml:mrow></mml:math 	:mml:mn>	∙2∛mml:mn
118	Allâ€ S oft and Stretchable Thermogalvanic Gel Fabric for Antideformity Body Heat Harvesting Wearable. Advanced Energy Materials, 2021, 11, 2102219.	10.2	52
119	Microstructure and Thermoelectric Properties of Mechanically Robust PbTe-Si Eutectic Composites. Chemistry of Materials, 2010, 22, 869-875.	3.2	50
120	Effective atomic interface engineering in Bi2Te2.7Se0.3 thermoelectric material by atomic-layer-deposition approach. Nano Energy, 2018, 49, 257-266.	8.2	49
121	Eutectoid nano-precipitates inducing remarkably enhanced thermoelectric performance in (Sn _{1â^'x} Cd _x Te) _{1â^'y} (Cu ₂ Te) _y . Journal of Materials Chemistry A, 2020, 8, 2798-2808.	5.2	49
122	Enhanced-Performance PEDOT:PSS/Cu ₂ Se-Based Composite Films for Wearable Thermoelectric Power Generators. ACS Applied Materials & Interfaces, 2021, 13, 631-638.	4.0	49
123	Exceptionally High Power Factor Ag ₂ Se/Se/Polypyrrole Composite Films for Flexible Thermoelectric Generators. Advanced Functional Materials, 2022, 32, 2106902.	7.8	49
124	Growth dynamics and strain relaxation mechanisms inBaTiO3pulsed laser deposited onSrRuO3â^•SrTiO3. Physical Review B, 2006, 73, .	1.1	48
125	Revisiting AgCrSe ₂ as a promising thermoelectric material. Physical Chemistry Chemical Physics, 2016, 18, 23872-23878.	1.3	48
126	Anomalous Electronic Transport in Dual-Nanostructured Lead Telluride. Journal of the American Chemical Society, 2011, 133, 8786-8789.	6.6	47

#	Article	IF	CITATIONS
127	Unexpected Large Hole Effective Masses in SnSe Revealed by Angle-Resolved Photoemission Spectroscopy. Physical Review Letters, 2017, 119, 116401.	2.9	47
128	High Performance and Flexible Polyvinylpyrrolidone/Ag/Ag ₂ Te Ternary Composite Film for Thermoelectric Power Generator. ACS Applied Materials & Interfaces, 2019, 11, 33254-33262.	4.0	47
129	Extraordinary Selectivity of CoMo ₃ S ₁₃ Chalcogel for C ₂ H ₆ and CO ₂ Adsorption. Advanced Materials, 2011, 23, 4857-4860.	11.1	46
130	Point Defect Engineering: Coâ€Doping Synergy Realizing Superior Performance in nâ€Type Bi ₂ Te ₃ Thermoelectric Materials. Small, 2021, 17, e2101328.	5.2	45
131	Metal Acetylacetonates as General Precursors for the Synthesis of Early Transition Metal Oxide Nanomaterials. Journal of Nanomaterials, 2007, 2007, 1-7.	1.5	44
132	Enhancing thermoelectric performance of SnTe via nanostructuring particle size. Journal of Alloys and Compounds, 2017, 709, 575-580.	2.8	44
133	Achieving an excellent thermoelectric performance in nanostructured copper sulfide bulk via a fast doping strategy. Materials Today Physics, 2019, 8, 71-77.	2.9	44
134	Hydrothermal degradation of cubic zirconia. Acta Materialia, 2003, 51, 5123-5130.	3.8	43
135	Strongly Nonlinear Optical Chalcogenide Thin Films of APSe ₆ (A=K, Rb) from Spin oating. Angewandte Chemie - International Edition, 2011, 50, 10867-10870.	7.2	43
136	Extremely Low Thermal Conductivity in Thermoelectric Ge _{0.55} Pb _{0.45} Te Solid Solutions via Se Substitution. Chemistry of Materials, 2016, 28, 6367-6373.	3.2	42
137	Magnetotransport signatures of Weyl physics and discrete scale invariance in the elemental semiconductor tellurium. Proceedings of the National Academy of Sciences of the United States of America, 2020, 117, 11337-11343.	3.3	42
138	Investigation into the extremely low thermal conductivity in Ba heavily doped BiCuSeO. Nano Energy, 2016, 27, 167-174.	8.2	40
139	Substrateless Welding of Self-Assembled Silver Nanowires at Air/Water Interface. ACS Applied Materials & Interfaces, 2016, 8, 20483-20490.	4.0	39
140	High Thermoelectric Performance through Crystal Symmetry Enhancement in Triply Doped Diamondoid Compound Cu ₂ SnSe ₃ . Advanced Energy Materials, 2021, 11, 2100661.	10.2	39
141	Sharp ferroelectric phase transition in strained single-crystalline SrRuO3/Ba0.7Sr0.3TiO3/SrRuO3 capacitors. Applied Physics Letters, 2003, 83, 5011-5013.	1.5	38
142	Role of Self-Organization, Nanostructuring, and Lattice Strain on Phonon Transport in NaPb _{18-<i>x</i>} Sn _{<i>x</i>} BiTe ₂₀ Thermoelectric Materials. Journal of the American Chemical Society, 2009, 131, 17828-17835.	6.6	38
143	Assessment of similarity relations using helium for prediction of hydrogen dispersion and safety in an enclosure. International Journal of Hydrogen Energy, 2016, 41, 15388-15398.	3.8	38
144	The Role of Electron–Phonon Interaction in Heavily Doped Fineâ€Grained Bulk Silicons as Thermoelectric Materials. Advanced Electronic Materials, 2016, 2, 1600171.	2.6	38

#	Article	IF	CITATIONS
145	Dynamic piezo-thermoelectric generator for simultaneously harvesting mechanical and thermal energies. Nano Energy, 2020, 69, 104397.	8.2	38
146	Enhancing thermoelectric performance of SnTe via stepwisely optimizing electrical and thermal transport properties. Journal of Alloys and Compounds, 2019, 773, 571-584.	2.8	37
147	Realizing Improved Thermoelectric Performance in Bil ₃ -Doped Sb ₂ Te ₃ (GeTe) ₁₇ via Introducing Dual Vacancy Defects. Chemistry of Materials, 2020, 32, 1693-1701.	3.2	36
148	Atomic origins of the strong metal–support interaction in silica supported catalysts. Chemical Science, 2021, 12, 12651-12660.	3.7	36
149	Carbon-Involved Near-Surface Evolution of Cobalt Nanocatalysts: An in Situ Study. CCS Chemistry, 2021, 3, 154-167.	4.6	36
150	Comparison of precursors for pulsed metal–organic chemical vapor deposition of HfO2 high-K dielectric thin films. Thin Solid Films, 2005, 478, 206-217.	0.8	35
151	Colloidal syntheses of zero-dimensional Cs ₄ SnX ₆ (X = Br, I) nanocrystals with high emission efficiencies. Chemical Communications, 2020, 56, 387-390.	2.2	35
152	Realizing high thermoelectric performance of polycrystalline SnS through optimizing carrier concentration and modifying band structure. Journal of Alloys and Compounds, 2019, 789, 485-492.	2.8	34
153	High Performance Polymer Thermoelectric Composite Achieved by Carbon-Coated Carbon Nanotubes Network. ACS Applied Energy Materials, 2019, 2, 2427-2434.	2.5	34
154	Highly enhanced thermoelectric properties of nanostructured Bi ₂ S ₃ bulk materials <i>via</i> carrier modification and multi-scale phonon scattering. Inorganic Chemistry Frontiers, 2019, 6, 1374-1381.	3.0	33
155	Investigations on distinct thermoelectric transport behaviors of Cu in n-type PbS. Journal of Alloys and Compounds, 2019, 781, 820-830.	2.8	32
156	Direct observation of a fully strained dead layer at Ba0.7Sr0.3TiO3â^•SrRuO3 interface. Applied Physics Letters, 2005, 87, 062901.	1.5	31
157	Integrating plasmonic nanostructures with natural photonic architectures in Pd-modified <i>Morpho</i> butterfly wings for sensitive hydrogen gas sensing. RSC Advances, 2018, 8, 32395-32400.	1.7	31
158	Solâ^'Gel-Derived Epitaxial Nanocomposite Thin Films with Large Sharp Magnetoelectric Effect. ACS Nano, 2010, 4, 6836-6842.	7.3	30
159	Dopant Distributions in PbTe-Based Thermoelectric Materials. Journal of Electronic Materials, 2012, 41, 1583-1588.	1.0	30
160	High-performance low-temperature magnetic refrigerants made of gadolinium-hydroxy-chloride. Journal of Materials Chemistry C, 2016, 4, 6473-6477.	2.7	30
161	Coherent Sb/CuTe Core/Shell Nanostructure with Large Strain Contrast Boosting the Thermoelectric Performance of nâ€Type PbTe. Advanced Functional Materials, 2021, 31, 2007340.	7.8	30
162	Interfacial reaction in the growth of epitaxial SrTiO3 thin films on (001) Si substrates. Journal of Applied Physics, 2005, 97, 104921.	1.1	29

#	Article	IF	CITATIONS
163	Competing two-phase coexistence in doped manganites: Direct observations byin situLorentz electron microscopy. Physical Review B, 2010, 82, .	1.1	29
164	Topotactic Redox Chemistry of NaFeAs in Water and Air and Superconducting Behavior with Stoichiometry Change. Chemistry of Materials, 2010, 22, 3916-3925.	3.2	29
165	Effect of silica shell thickness of Fe3O4–SiOx core–shell nanostructures on MRI contrast. Journal of Nanoparticle Research, 2013, 15, 1.	0.8	29
166	Butterfly Wing Hears Sound: Acoustic Detection Using Biophotonic Nanostructure. Nano Letters, 2019, 19, 2627-2633.	4.5	29
167	Remarkably enhanced thermoelectric properties of Bi2S3 nanocomposites via modulation doping and grain boundary engineering. Applied Surface Science, 2020, 520, 146341.	3.1	29
168	SnSe, the rising star thermoelectric material: a new paradigm in atomic blocks, building intriguing physical properties. Materials Horizons, 2021, 8, 1847-1865.	6.4	29
169	High thermoelectric performance of Ge1â~'xPbxSe0.5Te0.5 due to (Pb, Se) co-doping. Acta Materialia, 2014, 74, 215-223.	3.8	28
170	Aqueous gel casting of water-soluble calcia-based ceramic core for investment casting using epoxy resin as a binder. International Journal of Advanced Manufacturing Technology, 2016, 86, 1235-1242.	1.5	28
171	Attempting to realize n-type BiCuSeO. Journal of Solid State Chemistry, 2018, 258, 510-516.	1.4	28
172	N-type Bi-doped SnSe Thermoelectric Nanomaterials Synthesized by a Facile Solution Method. Inorganic Chemistry, 2018, 57, 13800-13808.	1.9	28
173	Rhodamine Mechanophore Functionalized Mechanochromic Double Network Hydrogels with High Sensitivity to Stress. Chinese Journal of Polymer Science (English Edition), 2020, 38, 24-36.	2.0	27
174	Dimer rattling mode induced low thermal conductivity in an excellent acoustic conductor. Nature Communications, 2020, 11, 5197.	5.8	27
175	Thermoelectric materials with crystal-amorphicity duality induced by large atomic size mismatch. Joule, 2021, 5, 1183-1195.	11.7	27
176	Realizing High Thermoelectric Performance in Earthâ€Abundant Bi ₂ S ₃ Bulk Materials via Halogen Acid Modulation. Advanced Functional Materials, 2021, 31, 2102838.	7.8	27
177	A highly asymmetric interfacial superstructure in WC: expanding the classic grain boundary segregation and new complexion theories. Materials Horizons, 2020, 7, 173-180.	6.4	26
178	Interfacial and microstructural properties of SrTiO3 thin films grown on Si(001) substrates. Journal of Applied Physics, 2002, 92, 7200-7205.	1.1	25
179	Realizing high figure of merit plateau in Ge Bi Te via enhanced Bi solution and Ge precipitation. Journal of Alloys and Compounds, 2019, 805, 831-839.	2.8	25
180	Step-Up Thermoelectric Performance Realized in Bi ₂ Te ₃ Alloyed GeTe via Carrier Concentration and Microstructure Modulations. ACS Applied Energy Materials, 2019, 2, 1616-1622.	2.5	25

#	Article	IF	CITATIONS
181	A novel 3D-printable hydrogel with high mechanical strength and shape memory properties. Journal of Materials Chemistry C, 2019, 7, 14913-14922.	2.7	25
182	Hydrothermal synthesis of SnQ (<i>Q</i> = Te, Se, S) and their thermoelectric properties. Nanotechnology, 2017, 28, 455707.	1.3	24
183	SnSeÂ+ÂAg2Se composite engineering with ball milling for enhanced thermoelectric performance. Rare Metals, 2018, 37, 333-342.	3.6	24
184	Achieving a fine balance between the strong mechanical and high thermoelectric properties of n-type PbTe–3% Sb materials by alloying with PbS. Journal of Materials Chemistry A, 2019, 7, 6304-6311.	5.2	24
185	Interfacial superstructures and chemical bonding transitions at metal-ceramic interfaces. Science Advances, 2021, 7, .	4.7	24
186	Microstructure and interfaces of HfO2 thin films grown on silicon substrates. Journal of Crystal Growth, 2004, 262, 295-303.	0.7	23
187	Large enhancement of electrical transport properties of SnS in the out-of-plane direction by n-type doping: a combined ARPES and DFT study. Journal of Materials Chemistry A, 2018, 6, 24588-24594.	5.2	22
188	Origin of the enhancement in transport properties on polycrystalline SnSe with compositing two-dimensional material MoSe ₂ . Nanotechnology, 2017, 28, 105708.	1.3	20
189	Achieving High Thermoelectric Performance in p-Type BST/PbSe Nanocomposites through the Scattering Engineering Strategy. ACS Applied Materials & Interfaces, 2020, 12, 46181-46189.	4.0	20
190	Strained Endotaxial PbS Nanoprecipitates Boosting Ultrahigh Thermoelectric Quality Factor in nâ€Type PbTe Asâ€Cast Ingots. Small, 2021, 17, e2104496.	5.2	20
191	Achieving high thermoelectric performance of Cu _{1.8} S composites with WSe ₂ nanoparticles. Nanotechnology, 2018, 29, 345402.	1.3	19
192	Highly enhanced thermoelectric performance in BiCuSeO ceramics realized by Pb doping and introducing Cu deficiencies. Journal of the American Ceramic Society, 2019, 102, 5989-5996.	1.9	19
193	Electric Polarization Switching on an Atomically Thin Metallic Oxide. Nano Letters, 2021, 21, 144-150.	4.5	19
194	Direct Atomicâ€6cale Structure and Electric Field Imaging of Triazineâ€Based Crystalline Carbon Nitride. Advanced Materials, 2021, 33, e2106359.	11.1	19
195	Microstructure and possible strain relaxation mechanisms of La2CuO4+δ thin films grown on LaSrAlO4 and SrTiO3 substrates. Journal of Applied Physics, 2007, 101, 073906.	1.1	18
196	Mechanical Alloying and Spark Plasma Sintering of BiCuSeO Oxyselenide: Synthesis Process and Thermoelectric Properties. Journal of the American Ceramic Society, 2016, 99, 507-514.	1.9	18
197	Investigation on thermal transport and structural properties of InFeO 3 (ZnO) m with modulated layer structures. Acta Materialia, 2017, 136, 235-241.	3.8	18
198	Design guidelines for chalcogenide-based flexible thermoelectric materials. Materials Advances, 2021, 2, 2584-2593.	2.6	18

#	Article	IF	CITATIONS
199	Enhanced Thermoelectric Performance Achieved in SnTe via the Synergy of Valence Band Regulation and Fermi Level Modulation. ACS Applied Materials & amp; Interfaces, 2021, 13, 50037-50045.	4.0	18
200	Self-supported hierarchical crystalline carbon nitride arrays with triazine-heptazine heterojunctions for highly efficient photoredox catalysis. Chemical Engineering Journal, 2022, 435, 134865.	6.6	18
201	Subtractive Structural Modification of <i>Morpho</i> Butterfly Wings. Small, 2015, 11, 5705-5711.	5.2	17
202	Thermoelectric properties of polycrystalline SnSe _{1±x} prepared by mechanical alloying and spark plasma sintering. RSC Advances, 2016, 6, 92335-92340.	1.7	17
203	Excellent Thermoelectric Performance Realized in p-Type Pseudolayered Sb ₂ Te ₃ (GeTe) ₁₂ via Rhenium Doping. ACS Applied Energy Materials, 2020. 3. 2063-2069. Scaled frequency-dependent transport in the mesoscopically phase-separated colossal	2.5	17
204	magnetoresistive manganite <mml:math <br="" xmlns:mml="http://www.w3.org/1998/Math/MathML">display="inline"><mml:mrow><mml:msub><mml:mi mathvariant="normal">La<mml:mrow><mml:mn>0.625</mml:mn><mml:mo>â^'</mml:mo><mml:mi mathvariant="normal">Pr<mml:mi>y</mml:mi></mml:mi </mml:mrow></mml:mi </mml:msub><mml:msub><mml:msub><mml:mi< td=""><td>>y<td>ni>{/mml:mrc</td></td></mml:mi<></mml:msub></mml:msub></mml:mrow></mml:math>	>y <td>ni>{/mml:mrc</td>	ni>{/mml:mrc
205	mathyariant="normal">Cacmml:mi mathvari. Physical Direct atomic-scale observation of the Ag ⁺ diffusion structure in the quasi-2D "liquid-like―state of superionic thermoelectric AgCrSe ₂ . Journal of Materials Chemistry C, 2019, 7, 9263-9269.	2.7	16
206	SrZrO3Nanopatterning Using Self-Organized SrRuO3as a Template. Advanced Materials, 2005, 17, 281-284.	11.1	15
207	Excellent thermoelectric performance achieved over broad temperature plateau in indium-doped SnTe-AgSbTe2 alloys. Applied Physics Letters, 2018, 112, .	1.5	15
208	Enhanced thermoelectric performance realized in AgBiS2 composited AgBiSe2 through indium doping and mechanical alloying. Applied Physics Letters, 2018, 112, .	1.5	15
209	High performance Ag2Se/Ag/PEDOT composite films for wearable thermoelectric power generators. Materials Today Physics, 2021, 21, 100553.	2.9	15
210	Synergy of Valence Band Modulation and Grain Boundary Engineering Leading to Improved Thermoelectric Performance in SnTe. ACS Applied Energy Materials, 2021, 4, 14608-14617.	2.5	15
211	Thermoelectric properties of Cu2Se prepared by solution phase methods and spark plasma sintering. Journal of the European Ceramic Society, 2017, 37, 4687-4692.	2.8	14
212	Influence of impurities on the conductivity of composites in the system (3YSZ)1â^'x–(MgO)x. Journal of Power Sources, 2005, 148, 32-42.	4.0	13
213	New nonhydrolytic route to synthesize crystalline BaTiO3 nanocrystals with surface capping ligands. Journal of Materials Research, 2006, 21, 3187-3195.	1.2	13
214	Research on Humidity Resistance of Sodium Silicate Sand Hardened by Twice Microwave Heating Process. Materials and Manufacturing Processes, 2014, 29, 184-187.	2.7	13
215	Microstructures of epitaxial La0.7Ca0.3MnO3 thin films grown on SrTiO3 and NdGaO3 substrates. Journal of Crystal Growth, 2004, 265, 241-249.	0.7	12
216	Understanding the effects of iodine doping on the thermoelectric performance of n-type PbTe ingot materials. Journal of Applied Physics, 2019, 126, .	1.1	12

#	Article	IF	CITATIONS
217	Enhanced thermoelectric performance in GeTe-Sb2Te3 pseudo-binary via lattice symmetry regulation and microstructure stabilization. Materials Today Physics, 2021, 21, 100507.	2.9	12
218	Controllable assembly of Pd nanosheets: a solution for 2D materials storage. CrystEngComm, 2017, 19, 3439-3444.	1.3	12
219	Excellent thermoelectric properties and stability realized in copper sulfides based composites via complex nanostructuring. Acta Materialia, 2022, 233, 117972.	3.8	12
220	Orthorhombic to Cubic Phase Transition in La1?xCaxMnO3 Perovskites. Physica Status Solidi (B): Basic Research, 2002, 229, 1145-1154.	0.7	11
221	Ferromagnetic domain structures and spin configurations measured in doped manganite. Physical Review B, 2010, 81, .	1.1	11
222	Electrical and thermal transport properties of layered Bi2YO4Cu2Se2. Journal of Solid State Chemistry, 2016, 239, 178-183.	1.4	11
223	Large enhancement of thermoelectric performance of InTe compound by sintering and CuInTe2 doping. Journal of Applied Physics, 2019, 126, .	1.1	11
224	Three-Dimensional Atom-Probe Tomographic Analyses of Lead-Telluride Based Thermoelectric Materials. Jom, 2014, 66, 2288-2297.	0.9	10
225	Highly Enhanced Thermoelectric and Mechanical Properties of Bi-Sb-Te Compounds by Carrier Modulation and Microstructure Adjustment. ACS Applied Materials & Interfaces, 2021, 13, 45589-45599.	4.0	10
226	Anisotropic Landau level splitting and Lifshitz transition induced magnetoresistance enhancement in ZrTe ₅ crystals. New Journal of Physics, 2019, 21, 093009.	1.2	9
227	High onductive Protonated Layered Oxides from H ₂ O Vaporâ€Annealed Brownmillerites. Advanced Materials, 2021, 33, e2104623.	11.1	9
228	Porous Thermoelectric Zintl: YbCd ₂ Sb ₂ . ACS Applied Energy Materials, 2021, 4, 913-920.	2.5	9
229	Microstructure of epitaxial Ba0.7Sr0.3TiO3â^•SrRuO3 bilayer films on SrTiO3 substrates. Journal of Applied Physics, 2005, 97, 104907.	1.1	8
230	Directing Gold Nanoparticles into Free‣tanding Honeycomb‣ike Ordered Mesoporous Superstructures. Small, 2019, 15, e1901304.	5.2	8
231	Antisite Defectâ€Enhanced Thermoelectric Performance of Topological Crystalline Insulators. Advanced Functional Materials, 2020, 30, 2003162.	7.8	8
232	Redesign high-performance flexible thermoelectrics: From mathematical algorithm to artificial cracks. Applied Physics Letters, 2020, 116, .	1.5	8
233	Significantly Enhanced Thermoelectric Performance Achieved in CuGaTe ₂ through Dual-Element Permutations at Cation Sites. ACS Applied Materials & Interfaces, 2022, 14, 30046-30055.	4.0	8
234	Diverging giant magnetoresistance in ferromagnet-superconductor-ferromagnet trilayers. Physical Review B, 2008, 78, .	1.1	7

#	Article	IF	CITATIONS
235	Coupling effects in 3D plasmonic structures templated by <i>Morpho</i> butterfly wings. Nanoscale, 2018, 10, 533-537.	2.8	7
236	GaP–ZnS Multilayer Films: Visible-Light Photoelectrodes by Interface Engineering. Journal of Physical Chemistry C, 2019, 123, 3336-3342.	1.5	7
237	Delocalized Carriers and the Electrical Transport Properties of n-Type GeSe Crystals. ACS Applied Energy Materials, 2019, 2, 3703-3707.	2.5	7
238	Butterfly Wing Inspired High Performance Infrared Detection with Spectral Selectivity. Advanced Optical Materials, 2020, 8, 1901647.	3.6	7
239	Nano-patterning of a monolayer molybdenum disulfide with sub-nanometer helium ion beam: considering its shape, size and damage. Nanotechnology, 2020, 31, 345302.	1.3	7
240	Pressure effects on the electrical transport and anharmonic lattice dynamics of r-GeTe: A first-principles study. Journal of Materiomics, 2021, 7, 1190-1197.	2.8	7
241	Realizing high thermoelectric performance in N-type Bi2Te3 compounds by Sb nano-precipitates. Journal of Applied Physics, 2021, 130, .	1.1	7
242	Geometric shadowing from rippledSrRuO3â^•SrTiO3surface templates induces self-organization of epitaxialSrZrO3nanowires. Physical Review B, 2006, 74, .	1.1	6
243	Structural origin of enhanced critical temperature in ultrafine multilayers of cuprate superconducting films. Physical Review B, 2014, 89, .	1.1	6
244	Understanding Phonon Scattering by Nanoprecipitates in Potassium-Doped Lead Chalcogenides. ACS Applied Materials & Interfaces, 2017, 9, 3686-3693.	4.0	6
245	Enhanced thermoelectric performance of heavy-fermion YbAl3 via multi-scale microstructures. Journal of Alloys and Compounds, 2017, 725, 1297-1303.	2.8	6
246	Three-dimensional Insight on Formation and Light-harvesting of Hollow-structure Carbon Nitride. ACS Applied Energy Materials, 2020, 3, 7020-7029.	2.5	6
247	Interfacial origins of visible-light photocatalytic activity in ZnS–GaP multilayers. Acta Materialia, 2019, 181, 139-147.	3.8	5
248	Enhanced thermoelectric properties in chimney ladder structured Mn(BxSi1-x)1.75 due to the dual lattice occupation of boron. Applied Physics Letters, 2019, 115, 123902.	1.5	5
249	Plasmonic evolution of atomically size-selected Au clusters by electron energy loss spectrum. National Science Review, 2020, 8, nwaa282.	4.6	5
250	Single-element amorphous palladium nanoparticles formed via phase separation. Nano Research, 2022, 15, 5575-5580.	5.8	5
251	Converting Brownmillerite to Alternate Layers of Oxygenâ€Deficient and Conductive Nanoâ€Sheets with Enhanced Thermoelectric Properties. Advanced Energy Materials, 2022, 12, .	10.2	5
252	Bioinspired infrared detection using thermoresponsive hydrogel nanoparticles. Pure and Applied Chemistry, 2015, 87, 1029-1038.	0.9	4

#	Article	IF	CITATIONS
253	Evolvement of microstructure and lattice thermal conductivity in Na doped PbTe–PbS pseudoâ^'binary system. Journal of Materiomics, 2016, 2, 150-157.	2.8	4
254	Visibleâ€lightâ€stimulated Alkalisâ€triggered Platinum Cocatalyst with Electron Deficient Interface for Hydrogen Evolution. ChemCatChem, 2020, 12, 2189-2193.	1.8	4
255	ZnS-GaP Solid Solution Thin Films with Enhanced Visible-Light Photocurrent. ACS Applied Energy Materials, 0, , .	2.5	4
256	Self-organization of epitaxial La0.35Pr0.275Ca0.375MnO3 manganite nanorods on NdGaO3 substrates. Journal of Applied Physics, 2008, 103, 064304.	1.1	3
257	Isolation and characterization of thirteen novel dinucleotide microsatellite loci from Tetraena mongolica Maxim. Conservation Genetics Resources, 2014, 6, 297-299.	0.4	3
258	Investigation of Solid-State Immiscibility and Thermoelectric Properties of the System PbTe – PbS. Materials Research Society Symposia Proceedings, 2009, 1166, 7.	0.1	2
259	Investigation of the thermoelectric properties of the PbTe-SrTe system. Materials Research Society Symposia Proceedings, 2010, 1267, 1.	0.1	2
260	Giant magneto-resistance estimated from direct observation of nanoscale ferromagnetic domain evolution in La0.325Pr0.3Ca0.375MnO3. Journal of Applied Physics, 2012, 112, 053924.	1.1	2
261	Thermoelectric Materials: Enhancement of Thermoelectric Figure of Merit by the Insertion of MgTe Nanostructures in <i>p</i> â€type PbTe Doped with Na ₂ Te (Adv. Energy Mater. 9/2012). Advanced Energy Materials, 2012, 2, 1038-1038.	10.2	2
262	Flash Solid–Solid Synthesis of Silicon Oxide Nanorods. Small, 2020, 16, 2001435.	5.2	2
263	Realizing High Thermoelectric Performance in Earthâ€Abundant Bi ₂ S ₃ Bulk Materials via Halogen Acid Modulation (Adv. Funct. Mater. 37/2021). Advanced Functional Materials, 2021, 31, 2170277.	7.8	2
264	Synergistic Strategies to Boost Lead Telluride as Prospective Thermoelectrics. , 2021, , 155-189.		2
265	Boosting the Thermoelectric Performance of Zinc blende-like Cu2SnSe3 through Phase Structure and Band Structure Regulations. Journal of Materials Chemistry A, 0, , .	5.2	2
266	Comparison of Hafnium Precursors for the MOCVD of HfO 2 for Gate Dielectric Applications. Integrated Ferroelectrics, 2003, 57, 1163-1173.	0.3	1
267	Thermoelectric Properties of Composite PbTe – PbSnS2 Materials. Materials Research Society Symposia Proceedings, 2010, 1267, 1.	0.1	1
268	Electron-beam activated thermal sputtering of thermoelectric materials. Journal of Applied Physics, 2011, 110, 044325.	1.1	1
269	Impact of crystalline structures on the thermal stability and Schottky barrier height of NiGe/Ge contact. Applied Physics Letters, 2018, 113, 253503.	1.5	1
270	Bioinspired Color Change through Guided Reflection. Advanced Optical Materials, 2018, 6, 1800464.	3.6	1

#	Article	IF	CITATIONS
271	Vapor detection through dynamic process of molecule desorption from butterfly wings. Pure and Applied Chemistry, 2020, 92, 223-232.	0.9	1
272	Orthorhombic to Cubic Phase Transition in La1â \in "xCaxMnO3 Perovskites. , 2002, 229, 1145.		1
273	Site determination of Mn atoms in Sn-Mn-Te alloy by electron channeling enhanced microanalysis. Applied Physics Letters, 2021, 119, 243906.	1.5	1
274	Domain structures and superdislocations of La0.7Ca0.3MnO3 thin films grown on SrTiO3 substrates. Journal of Crystal Growth, 2007, 306, 437-443.	0.7	0
275	Understanding Electrical Transport and the Large Power Factor Enhancements in Co-Nanostructured PbTe. Materials Research Society Symposia Proceedings, 2009, 1166, 1.	0.1	0
276	Characterization of PbTe-based Thermoelectric Materials by Scanning/ Transmission Electron Microscopy (S/TEM). Microscopy and Microanalysis, 2009, 15, 1400-1401.	0.2	0
277	Electron Microscopy for Characterization of Thermoelectric Nanomaterials. , 2014, , 427-536.		0
278	Electro-interconverted thermogelling and thermothinning polymer solutions. Polymer Chemistry, 2018, 9, 5303-5307.	1.9	0
279	Superstructures: Directing Gold Nanoparticles into Freeâ€Standing Honeycombâ€Like Ordered Mesoporous Superstructures (Small 31/2019). Small, 2019, 15, 1970165.	5.2	0
280	A COMBINATION OF POINT DEFECTS AND NANOSIZED GRAINS TO MINIMIZE LATTICE THERMAL CONDUCTIVITY OF Sn AND Se CO-DOPED CoSb ₃ VIA MIXED BALL MILLING AND SPARK PLASMA SINTERING. Surface Review and Letters, 2021, 28, .	0.5	0
281	Surface Crystallization of Amorphous Palladium Nanoparticles. Journal of Physical Chemistry C, 2021, 125, 1107-1112.	1.5	0